



1 **Comparison of in-situ snow depth measurements and impacts**
2 **on validation of unpiloted aerial system lidar over a mixed-use**
3 **temperate forest landscape**

4

5 Holly Proulx¹, Jennifer M. Jacobs^{1,2}, Elizabeth A. Burakowski², Eunsang Cho^{1,2}, Adam G.
6 Hunsaker^{1,2}, Franklin B. Sullivan², Michael Palace^{2,3}, Cameron Wagner¹

7 ¹Department of Civil and Environmental Engineering, University of New Hampshire, Durham, NH, 03824, USA

8 ²Earth Systems Research Center, Institute for the Study of Earth, Oceans, and Space, University of New
9 Hampshire, Durham, NH, 03824, USA

10 ³Department of Earth Sciences, University of New Hampshire, Durham, NH, 03824, USA

11 *Correspondence to:* Jennifer M. Jacobs (Jennifer.jacobs@unh.edu)

12 **Abstract.** The accuracy and consistency of snow depth measurements depend on the measuring device and the
13 conditions of the site and snowpack in which it is being used. This study compares collocated snow depth
14 measurements from a magnaprobe automatic snow depth probe and a Federal snow tube, then uses these
15 measurements to validate snow depth maps from an unpiloted aerial system (UAS) with an integrated Light
16 Detection and Ranging (lidar) sensor. We conducted three snow depth sampling campaigns from December 2020
17 to February 2021 that included 39 open field, coniferous, mixed, and deciduous forest sampling sites in Durham,
18 New Hampshire, United States. Average snow depths were between 9 and 15 cm. For all sampling campaigns and
19 land cover types, the magnaprobe snow depth measurements were consistently deeper than the snow tube. There
20 was a 12% average difference between the magnaprobe (14.9 cm) and snow tube (13.2 cm) average snow depths
21 with a greater difference in the forest than the field. The lidar estimates of snow depth were 3.6 cm and 1.9 cm
22 shallower on average than the magnaprobe and snow tube, respectively. While the magnaprobe had a better
23 correlation with the UAS lidar, the root mean square errors were higher for the magnaprobe than the snow tube,
24 likely due to overprobing by the magnaprobe into leaf litter. Even though the differences between the in-situ
25 sampling methods resulted in modest performance differences when used to validate the UAS lidar snow depths
26 in this study, measuring vegetation height, leaf litter, and soil frost with in-situ snow depths from multiple
27 sampling techniques helped to account for the errors of in-situ snow depth for robust validation of the UAS snow
28 depth maps.

29

30 **Short Summary.** This study compares snow depth measurements from two manual instruments and an airborne
31 platform in a field and forest. The manual instruments' snow depths differed by 1 to 3 cm. The airborne
32 measurements, which do not penetrate the leaf litter, were consistently shallower than either manual instrument.
33 When combining airborne snow depth maps with manual density measurements, corrections may be required to
34 create unbiased maps of snow properties.

35 **1 Introduction**

36 Snow depth is the most commonly measured snow macrophysical property followed by snow presence, snow
37 water equivalent (SWE) and snow bulk density (Pirazzini et al. 2018). While snowpack conditions are important



38 to both research and operations, it is still challenging to obtain measurements. Snow depth is the easiest snowpack
39 property to measure in the field and is considered to be an observation that can be measured relatively precisely
40 without considerable expertise or expense. Hundreds of snow depth measurements can readily be taken in a single
41 day and automated samplers can considerably increase that number (Sturm and Holmgren 2018). Sturm et al.
42 (2010) estimated that 20 to 30 snow depth measurements can be made in the time it takes to obtain a single SWE
43 measurement. Because snow depth is assumed to have greater spatial variability than snow density (Elder et al.
44 1998), numerous snow depth measurements are often made per snow density measurement then combined to
45 obtain SWE (López-Moreno et al. 2013). A snow survey usually includes both gravimetric SWE sampling and
46 snow depth measurements collected over a large area; a technique is referred to as “double sampling” (Derry et al.
47 2009; Rovaneck et al. 1993). Additionally, estimating SWE from snow depth is considerably easier than
48 measuring SWE using snow density from snow tubes measurements. Jonas et al. (2009) and Sturm et al. (2010)
49 developed simple methods to predict the bulk density and, in turn, SWE, based on snow depth measurements, the
50 day of the year, and snow class, thus entirely eliminating the need to make bulk density measurements.
51 Subsequently, others have tested and advanced approaches to predict the bulk density and estimate SWE
52 (Guyennon et al. 2019; Hill et al. 2019).

53

54 As reviewed by Kinar and Pomeroy (2015) and Kopp et al. (2019), there are various methods to observe snow
55 depth including (1) traditional in-situ observations, (2) non-destructive radar, lidar, and Structure from Motion
56 (SfM) methods, and (3) satellite remote sensing. The latter two methods, which improve the spatial coverage,
57 typically still rely on in-situ snow depth measurements for calibration of operational technique and validating
58 remotely sensed observations and model output. Traditional in-situ observations can be measured manually or
59 automatically. While automated measurements using ultrasonic, laser depth sensors, or time-lapse cameras in
60 combination with measuring rods are increasing in popularity (Kinar and Pomeroy 2015) (Kopp et al. 2019), in-
61 situ measurements remain a mainstay of research and operations (Kinar and Pomeroy 2015; Pirazzini et al. 2018).

62

63 Manual in-situ snow depth measurements are typically made using snow stakes, rulers, or narrow diameter snow
64 probes (Kinar and Pomeroy 2015; Pirazzini et al. 2018). Snow tube samplers, which have been in use since the
65 1930s, also measure snow depth because SWE is the product of snow depth and the depth averaged snowpack
66 density. The magnaprobe, an automatic snow depth probe that records snow depth and GPS measurements, has
67 considerably increased the number of georeferenced snow depth observations that can be made in a single day
68 and is used extensively for snow depth research campaigns (Sturm and Holmgren 2018; Walker et al. 2020). For
69 these snow depth measurements, the probe is manually pushed through the snow until it hits ground, while the
70 magnetostrictive basket floats on the snow surface; at the push of a button, the magnaprobe automatically records
71 the distance between the probe tip and basket. Measurement variability and errors are sometimes reduced by
72 repeating the measurement, typically three times (Leppänen et al. 2016).

73

74 SWE measurement errors associated with snow tube samplers are relatively well understood. Known issues
75 include biases as compared to snow pit measurements (Dixon and Boon, 2012; Farnes et al., 1983; Goodison,
76 1978; Sturm et al., 2010), accuracies around +/- 5% to 10% for an individual instrument, and differences among
77 SWE from different snow tube models (e.g., the Meteorological Service of Canada, the Federal or Mt. Rose, the



78 Adirondack, and the Snow-Hydro) that can exceed 10% (Farnes et al. 1983). These errors are attributed to issues
79 in obtaining the correct snow weight due to over- or under-sampling of snow in the core tube and accuracies in
80 spring or digital balances used to weigh the core.
81

82 As compared to snow tube samplers, much less is understood about the errors in snow depth measurements using
83 snow probes and differences among commonly used measurement techniques. The magnaprobe, which measures
84 snow depth with a precision of less than 0.1 mm, has the potential for low biases if its basket settles into soft
85 surface snow (cratering), but those biases are typically less than 1 cm (Sturm and Holmgren 2018). High biases
86 occur if a snow probe is inserted off vertically or the rod penetrates the substrate (overprobing) (Sturm and
87 Holmgren 2018). For the former case, reasonable operation will typically insert a rod within 5° of vertical and
88 result in an error of less than 0.4%, or 0.2 cm for 50 cm deep snow (Sturm and Holmgren 2018). For overprobing,
89 the error depends on the ground surface and the operation. Solid or frozen ground surfaces have negligible
90 overprobing. However, unfrozen natural surfaces may have considerable penetration (Derry et al. 2009) with
91 typical biases on the order of 5 to 10 cm (Berezovskaya and Kane 2007; Sturm and Holmgren 2018). Berezovskaya
92 and Kane (2007) estimate that snow depth errors cause SWE overestimates of 4 to 20% in northern Alaska.
93

94 Emerging remote-sensing methods, terrestrial laser scanning (TLS) (Currier et al. 2019; Grünewald and Lehning
95 2015), Unpiloted Aerial System (UAS) SfM (Bühler et al. 2016; Harder et al. 2016; Nolan et al. 2015), and UAS
96 lidar (Harder et al. 2020; Jacobs et al. 2021), can measure snow depth to within a centimeter at high spatial
97 resolutions. However, validation of those observations is challenging. For example, snow depth observations from
98 TLS and UAS lidar measurements are biased lower than those from in-situ snow probe observations in the forest
99 (Currier et al. 2019; Harder et al. 2020; Hopkinson et al. 2004; Jacobs et al. 2021). The causes of these differences
100 have been partially attributed to the snow probe's ability to penetrate the soil and vegetation and to human
101 observers who tend to make snow depth measurements in locations with relatively high snow (Sturm and
102 Holmgren 2018). Results from the comparison between snow depths measured using UAS lidar and a magnaprobe
103 (Jacobs et al. 2021) implied that the magnaprobe biases were greater than those taken using the Standard Federal
104 snow tube. Their work suggests that using the Federal snow tube snow depth measurements to validate UAS snow
105 depth products might be preferable to using magnaprobe measurements.
106

107 The goal of this brief study is to determine 1) if the magnitude of the snow depth measurements using a
108 magnaprobe and a Federal tube are significantly different in an ephemeral snow environment, 2) if the differences
109 vary by land cover type, 3) the magnitude of forest leaf litter impacts relative to any snow depth differences, and
110 4) how the two measuring techniques impact UAS lidar snow depth validation. Towards that end, we conducted
111 three snow depth sampling campaigns from December 2020 to March 2021 over field and forest plots at
112 Thompson Farm in Durham, New Hampshire, USA. The discussion below describes the results of these
113 experiments.



114 2 Site, Data, and Methods

115 2.1 Study Site

116 This study was conducted at the University of New Hampshire's Thompson Farm Research Observatory in
117 southeast New Hampshire, United States (N 43.11°, W 70.95°, 35 m above sea level, ASL). The 0.83 km² site has
118 mixed hardwood forest and open field land covers (Burakowski et al. 2018; Burakowski et al. 2015; Perron et al.
119 2004) that are characteristic of the region (Fig. 1). The agricultural fields are managed pasture grass with unmown
120 grass in local areas. The deciduous, mixed, and coniferous forest is composed primarily of white pine (*Pinus*
121 *strobus*), northern red oak (*Quercus rubra*), red maple (*Acer rubrum*), shagbark hickory (*Carya ovata*), and white
122 oak (*Quercus alba*) (Perron et al. 2004). The forest soils are classified as Hollis/Charlton very stony-fine sandy
123 loam and well-drained; field soils are characterized as Scantic silt-loam and poorly drained (Cho et al. 2021;
124 Perron et al. 2004).

125

126 In-situ sampling was conducted at 39 sites located along three parallel transects (Fig. 1). The approximately 145
127 m long transects were laid out from east to west. The transects were separated by approximately 10 m, north to
128 south. From east to west, each transect started in the open field area, then transitioned to the coniferous, then
129 mixed, and finally, deciduous forested areas. Each of the three transects had 13 sampling sites, four sites were in
130 the open field area, three in the coniferous forest, three in the mixed forest, and three in the deciduous forest, that
131 were marked with a stake. The stake locations were geolocated using a Trimble[®] Geo7X GNSS Positioning Unit
132 and Zephyr[™] antenna with an estimated horizontal uncertainty of 2.51 cm (standard deviation 0.95 cm) and 4.17
133 cm (standard deviation 4.60 cm) for the field and forest respectively after differential correction. Three Cold
134 Regions Research and Engineering Laboratory-Gandahl (CRREL-Gandahl) soil frost tubes (Gandahl 1957;
135 Rickard and Brown 1972; Sharratt and McCool 2005) were located in the field and forest approximately 25 m
136 south of the field transect. UAS lidar surveys were conducted over approximately an 0.2 km² area that
137 encompassed the transects.

138 2.2 In-Situ Sampling Methods

139 Snow depth was measured using a magnaprobe and a Federal snow sampler, also known as a snow tube. The
140 Federal snow tube with its long operational history (Clyde 1932) served as a historical reference against the
141 magnaprobe. A magnaprobe consists of an avalanche probe-like rod of about 1.5 m in length that contains a
142 magnetostrictive device and a sliding magnetic disk-shaped basket with a 25 cm diameter. The rod has a 1.27 cm
143 diameter with an affixed tip that tapers to a point to help penetrate ice layers. The magnaprobe was operated by
144 inserting the pole into a snowpack until the tip of the pole reached the ground surface, allowing the basket to slide
145 down to float on top of the snow. A handheld portable keypad connected to a datalogger recorded the snow depth
146 between the tip of the pole and the bottom of the basket.

147

148 A Federal snow sampler is an aluminum tube, about 76 cm in length with a 4.13 cm inner diameter, that is used
149 to measure snow depth and SWE (Clyde 1932). To measure snow depth, the snow tube was inserted vertically
150 into the snowpack until it reached the ground, and a depth was read at eye level. Snow depth was recorded to the
151 nearest 0.5 cm. To measure SWE, the snow tube was then lifted out of the snowpack, using a spatula as needed
152 to ensure that snow did not fall out of the tube. The snow and snow tube were weighed using a digital hanging



153 scale (CCI HS-6 Electronic Scale, 2 gram resolution). Snow mass was the total mass net of the empty tube mass.
154 Snow density was determined from the snow mass and sampled volume.

155

156 Sampling campaigns were conducted on 18 December 2020, 4 February 2021, and 24 February 2021. A total of
157 351 paired magnaprobe and Federal snow tube snow depth observations were collected during each campaign. At
158 each of the 39 sampling locations, nine measurements were made in a 1m x1 m area. Previous UAS lidar snow
159 depth precision analyses indicated that snow depth differences of 1 cm or less could be detected in a 1x1 m area
160 using nine samples for most of the study area (Jacobs et al. 2021). At each location, a 1x1 m square polyvinyl
161 chloride (PVC) grid was placed on the snow surface with one vertex located coincident with a stake. The
162 orientation of two adjacent sides of the grid was recorded. Nine magnaprobe depth measurements were made at
163 an approximately even spacing within the 1x1 m grid. Immediately after the magnaprobe measurements, snow
164 tube snow depth measurements were made at the same nine locations by positioning the snow tube directly over
165 each magnaprobe sampling location. At a 10th location within each 1x1 m grid, the snow tube was used to make
166 a SWE measurement. For the 24 February 2021 campaign, after the magnaprobe measurements were completed
167 for the two northern transects, the instrument was transferred to a new operator who made measurements on the
168 southernmost transect (Transect 1). The QA/QC process identified notable errors for observations from that
169 transect. Transect 1 data for that date were removed from the analysis.

170

171 Moultrie Wingscapes Birdcam Pro Field Cameras were used to capture images of the snowpack relative to a 1.5
172 meter marked PVC pole following the method used in NASA's 2020 SnowEx field camera campaign in Grand
173 Mesa, CO (personal communication, 16 November 2020). Three cameras were used; one was in the open field,
174 one was in the coniferous forest, and one was in the deciduous forest (**Fig. 1**). Each camera was mounted
175 approximately 0.85 m above the ground and placed approximately 5.5 m from its respective PVC pole. Each
176 camera's field of view included the entirety of the PVC pole, some of the ground surface below the pole, and
177 some open area above the pole. Each PVC pole was spray-painted red and was marked with 1 cm and 10 cm
178 increments. The cameras captured images of the poles every 15-minutes for the duration of the study period. Snow
179 depth was derived by manual inspection of the photos and recorded to the nearest cm.

180 **2.3 Ancillary Soils and Vegetation Cover Data**

181 2.3.1. Soil Frost

182 Daily soil frost depth data were collected at field and forest locations at the Thompson Farm Research Observatory
183 using (CRREL-Gandahl) style frost tubes (Gandahl 1957). The frost tubes have flexible, polyethylene inner tubing
184 filled with methylene blue dye whose color change is easy to differentiate when extruded from ice (Gandahl 1957;
185 Rickard and Brown 1972; Sharratt and McCool 2005). The outer tubing consists of PVC pipe installed between
186 0.4 to 0.5 m below the soil surface (Ricard et al. 1976; Sharratt and McCool 2005). The field and forest sites each
187 had three soil frost tubes. The average soil frost depth at the field and forest sites was calculated for each sampling
188 day.

189



190 2.3.2. Leaf Litter

191 Leaf litter depth was measured on 2 April 2021 after the spring snowmelt. The leaf litter depth was measured at
192 each snow depth sample location. Sampling was conducted using a PVC collar or round ring that is 8 cm in depth
193 and 10 cm in diameter (Kaspari and Yanoviak 2008). The collar was placed in the leaf litter and was pushed down
194 until it was through the leaf litter layer. If sticks or larger stones were in the way, they were either carefully
195 removed or the collar was moved slightly to an adjacent location. Measurements were taken using a wooden ruler
196 at four cardinal points in the collar. The four measurements were recorded and averaged, and the final litter depth
197 value was recorded to the nearest cm.

198

199 Magnaprobe penetration depth measurements were also made when snow was not present to capture the probe's
200 penetration into the leaf litter. Directly following the 2 April 2021 leaf litter sampling using the collar, 20
201 magnaprobe leaf litter depth measurements were made at each of the 39 snow depth sampling locations.
202 Measurements were taken within a 1.5 m radius of the stake. When using the magnaprobe, the weight of the probe
203 was the only force applied on the ground to minimize penetration into the duff layer and underlying soil. The
204 probe was gently rested on the ground rather than being forced into the ground. The 20 measurements were
205 recorded and averaged to obtain a magnaprobe litter depth at each location.

206 **2.4 Lidar Sampling**

207 UAS snow-on lidar surveys were conducted at Thompson Farm prior to in-situ sampling on each of the campaign
208 dates. A snow-off baseline survey was conducted on 2 April 2021 following snowmelt. The sensor payload
209 consisted of the Velodyne VLP-16 laser scanner, and the Applanix APX-15 Inertial Navigation System (INS;
210 GPS+IMU). The VLP-16 is a lightweight (~830 grams) low power (~8W) sensor, which makes it ideal for UAS
211 deployment. The sensor incorporates 16 rotating IR lasers that are arranged and oriented on the payload to provide
212 a 30° along-track field of view with a cross-track field of view limited only by the range of the sensor
213 (approximately 100 m). At an altitude of 65 m, the range of the sensor produces an effective cross-track field of
214 view of approximately 98°, but varies depending on the characteristics of the target surface. Each laser operates
215 at a wavelength of 903 nm. This wavelength is ideal because it is outside of the first major electromagnetic
216 absorption feature of snow (centered at 1030 nm). A reduction in signal strength would be observed over snow
217 cover for lidar sensors that operate at wavelengths coinciding with strong electromagnetic absorption. The VLP-
218 16 has two return modes, single-return and dual-return, which record the strongest return or the strongest and the
219 last return, respectively. In dual-return mode, the VLP-16 collects ~300,000 distance measurements per second
220 with a reported uncertainty of 3 cm at a range of 100 m.

221

222 For these acquisition missions, the VLP-16 was hard-mounted to a DJI Matrice 600 to maintain constant lever
223 arm offsets between the inertial navigation system (INS) GPS antenna, the lidar sensor, and the INS board. As
224 opposed to a gimbal mounted system, this hard-mounted configuration achieves a more tightly coupled system,
225 resulting in improved point cloud geolocation accuracy. The lidar sensor was set to dual-return mode to improve
226 ground detection in the forested areas of our field site. We flew the system at an altitude of 65 m with a flight
227 speed of 3 m/s and ~40 m spacing between flight lines. Flights produced between a total of ~70-140 million returns
228 per mission, depending on site ground conditions.



229

230 Lidar observations were georeferenced using position and attitude measurements acquired with the Applanix
231 APX-15 Inertial Navigation System (INS). The INS produced 2–5 cm positional, 0.025 degree roll and pitch, and
232 0.08 degree true heading uncertainties following post-processing. Post-processing of INS data was performed
233 using POSPac UAV (v. 8.2.1, Applanix Corporation 2018), correcting differentially against a permanent
234 Continuously Operating Reference Station (CORS) at the University of New Hampshire in Durham, NH (NHUN).
235 Position and attitude data were output as a Smoothed Best Estimate of Trajectory (SBET), then time synchronized
236 with lidar returns to produce a georeferenced point cloud using LidarTools (v. 3.1.4, Headwall Photonics, Inc.).

237

238 Three-dimensional point clouds were processed using the progressive morphological filter algorithm (PMF) to
239 identify ground returns. For ground classification, point clouds were chunked into 100 m square tiles with a 15 m
240 buffer on all sides using catalog options in lidR to ensure returns near tile edges were classified. PMF was
241 parameterized using a set of window sizes of 1, 3, 5, and 9 m, and elevation thresholds of 0.2, 1.5, 3, and 7 m,
242 which were determined by varying value sets and assessing digital terrain models (DTMs) to determine the
243 parameter sets that produced a visually smooth surface over a dense grid (Muir et al. 2017). Following ground
244 classification for each tile, returns within the 15 m tile buffers were removed, and all resulting 100 m square
245 ground classified tiles were merged. The result of the PMF is that non-ground returns (i.e., trees, shrubs, and
246 noise) were filtered out of the point cloud data sets, so that only returns from ground surfaces remained. The two
247 data sets, non-ground returns and ground returns from the original point clouds, were coded according to LAS
248 specifications and merged. The ground returns were extracted for the 1 x 1 m square sampling sites, corresponding
249 to the alignment and orientation of the respective PVC grids. The lidar snow depth was calculated as the difference
250 between the mean snow-on and mean snow-off elevations within each sampling grid.

251 2.5 Statistical Approach

252 The magnaprobe, snow tube, and lidar snow depth measurements were summarized and compared for the field
253 and forested areas by sampling campaign date following (Willmott 1982). Each comparison was conducted using
254 the individual grid cell measurements ($N = 9$ at each grid cell), and grid cell average depths. Sample statistics that
255 were calculated and compared for each of these datasets included the mean and standard deviation, the bias, the
256 mean absolute error (MAE), and the root mean square error (RMSE). A line of best fit was generated for each to
257 provide the corresponding slopes and intercepts, and r-squared values. As described by Willmott (1982), MAE of
258 the compared data sets, is given as:

$$259 \quad MAE = N^{-1} \sum_{i=1}^N |X_i - Y_i| \quad (1)$$

260

261 where X and Y are two of the magnaprobe, snow tube, and lidar snow depth and N is the number of samples. The
262 root mean square error (RMSE) is the average squared difference between the compared data sets given as:

$$263 \quad RMSE = [(N^{-1}) \sum_{i=1}^N (X_i - Y_i)^2]^{0.5} \quad (2)$$

264

265 The mean difference between snow depth from two sampling techniques quantifies the bias between the
266 measurements and, in doing so, identifies whether one sampling technique yields deeper or shallower snow on
267 average than another technique. The standard deviation characterizes the variability of those individual



268 differences. Ideally, measurements from the two instruments would have little to no systematic bias and the snow
269 depth differences would be relatively consistent at each sampling location. The RMSE of the snow depth
270 differences combines bias and variability into a single metric. Finally, significance tests of the mean snow depth
271 differences were conducted for each grid cell using t-tests after testing the normality of the data. The 24 February
272 2021 campaign, in which all measurements from Transect 1 were omitted from the dataset due to sampling errors,
273 had a lower sample size than other sampling campaign dates.

274 3 Results and Discussion

275 **Table 1** summarizes the snow and soil conditions by sampling campaign. Between the December and the 4
276 February sampling campaigns, there was a melt event during mid-December in which the entire snowpack ablated.
277 The next significant snowfall event (15 cm) occurred on 1 February 2021. The snowpack experienced little
278 additional accumulation or ablation between 4 February and 24 February. The field camera observations indicate
279 that the snowpacks had similar depths, between 10 and 15 cm, on the three sampling dates with modestly deeper
280 snow in the field than the forest. The February snowpack density values ($0.15 - 0.24 \text{ g/cm}^3$) were higher than
281 those in December ($\sim 0.10 \text{ g/cm}^3$). There was limited soil frost ($< 4 \text{ cm}$) during the early winter December
282 campaign in the forest and the field. The deepest soil frost was on 4 February 2021 with 15.1 cm in the field and
283 5.9 cm in the forest, with similar soil frost conditions on 24 February 2021.

284 3.1 Magnaprobe vs. Snow Tube

285 The full experiment yielded individual 936 pairs of snow depth measurements from the snow tube and the
286 magnaprobe (**Fig. 2a**). Overall, there was moderate agreement ($R^2 = 0.55$) between the two datasets for all three
287 sampling campaigns (**Table 2**). The snow depths measured by the magnaprobe (14.9 cm average snow depth)
288 were deeper than the snow tube (13.2 cm average snow depth) with an overall bias of 1.7 cm. The magnaprobe
289 snow depth was at least 0.5 cm deeper than the snow tube in 74% of the 936 measurement pairs. Only 6.3% of
290 the pairs had snow tube snow depths exceeding magnaprobe snow depths by 0.5 cm or more. 7.4% of the pairs'
291 magnaprobe snow depths were over 5.0 cm deeper than the snow tube. In eight pairs of measurements, the
292 magnaprobe snow depth was more than double the snow tube snow depth.

293

294 Out of the nine paired sampling locations in each grid, the majority (an average of 8.7, 7.7, and 7.0 of the sampling
295 locations in each grid on 18 December 2020, 4 and 24 February 2021, respectively) had magnaprobe snow depth
296 values that were deeper than those measured using the snow tube. The magnaprobe snow depth values were
297 significantly greater than those measured using the snow tube for 39 and 31 of the 39 sampling locations on 18
298 December 2020 and 4 February 2021, respectively, but only 11 out of the 26 sampling locations on 24 February
299 2021. The mean differences were 2.3, 1.4, and 1.6 cm, with RMSE values of 3.0, 2.3, and 3.3 cm, on 18 December
300 2020, 4 and 24 February 2021, respectively, which is on the order of 15 to 25% of the overall depth observed
301 during these campaigns. Despite the biases, the average within cell snow depth variability was nearly identical
302 for the magnaprobe and the snow tube in the field (1.3 cm standard deviation for the magnaprobe). In the forest,
303 the magnaprobe's 2.0 cm within cell standard deviation modestly exceeded the snow tube's 1.5 cm standard



304 deviation. The slightly reduced agreement on 2/24 may be due to a 1-4 cm thick ice layer at the bottom of the
305 snowpack in local depressions.

306

307 The overall agreement between the snow tube and magnaprobe was better when the nine measurements within a
308 single 1x1 m grid cell were averaged at each of the sampling locations (**Fig. 2b** and **Table 2**). There is a notable
309 improvement in grid cell statistics, and the correlation is stronger (overall $R^2 = 0.76$), with slopes closer to one,
310 intercepts closer to zero, and the RMSE values reduced to 2.5 cm or less. Although averaging has no impact on
311 the overall bias, the range of differences among pairs narrowed. Boxplots show that there is a consistent difference
312 (magnaprobe minus snow tube) that is typically constrained to less than 3 cm, but that a limited number of outliers
313 were observed (**Fig. 3b**). The magnaprobe snow depth was at least 0.5 cm deeper than the snow tube in almost all
314 grid cells (86.7%), but only three grid cells had differences greater than 5 cm. There were no instances in which
315 there was a doubling of snow depth.

316 **3.2 Magnaprobe vs. Snow Tube by Land type**

317 The magnaprobe and snow tube snow depths differ by land type, with the field having deeper snow and more
318 spatial variability than the forest land types (**Fig. 4**). Among the three forest types, the deepest snow was in the
319 deciduous-dominated forest, with mixed and coniferous forest having similar snow depths. The mean difference
320 between the magnaprobe and snow tube snow depths is a modest 1.3 cm in the field and a 1.9 cm in the forest,
321 with differences of 1.9, 2.0, and 1.9 cm in the deciduous, mixed, and coniferous land types, respectively. Based
322 on t-test results, the magnaprobe measured significantly deeper snow depth compared to the snow tube in both the
323 field and the forest. The t-test results identified significant differences between snow depths from the two probing
324 techniques regardless of whether individual locations (p -value < 0.001) or grid cell average snow depths (p -value
325 $= 0.02$) were used. Based on Welch's adjusted ANOVA test, there are no significant differences in overprobing
326 among forest land types (p -value $= 0.24$). The RMSE values between the magnaprobe and snow tube snow depths
327 are 3.0 cm (2.3 cm) and 2.5 cm (2.0 cm) for the forest and field sampling sites (grid average values), respectively.
328 Thus, the sampling method has a different impact in the field than the forest and the RMSE and bias values provide
329 an indicator of the different errors associated with in-situ measurements based on land type when used for model
330 or remote sensing validation.

331 **3.3 Impacts of Leaf Litter on Magnaprobe vs. Snow Tube Depth**

332 The range of leaf litter depths measured in the forest using the collar was typically 3 to 7 cm with an average leaf
333 litter depth of 3.9 cm (**Fig. 5**). The snow-off magnaprobe litter depth measurements in the forest had an average
334 value of 5.8 cm and the differences were significantly larger than depths measured using the collar (p -value $<$
335 0.001). The litter depths in the forest regardless of measurement technique exceeded the differences between the
336 magnaprobe and snow tube snow depths in the forest, which were 2.5, 1.7, and 1.4 cm on 18 December, 4
337 February, and 24 February, respectively.

338 **3.4 Lidar and *In-Situ* Snow Depth Comparison**

339 While the previous sections identified significant differences between the magnaprobe and snow tube snow
340 depth measurements, the average differences, 1.3 and 1.9 cm in the field and forest, respectively, are



341 relatively modest. One of the motivations for this study was to understand the impact of those differences
342 on the validation of emerging high resolution snow depth datasets such as those from UAS SfM or lidar
343 observations. Here, we briefly examine the lidar snow depth performance relative to both in-situ sampling
344 techniques and land type (**Table 3** and **Fig. 6**), then discuss the impact of different sampling techniques on
345 that evaluation.

346

347 The lidar-derived snow depths for each of the 1x1 m grid cells were extracted as described in Section 2.2.
348 For both magnaprobe and snow tube measurements, the agreement with lidar is markedly better in the field
349 than the forest (**Fig. 6**). Overall, the lidar estimates of snow depth are typically shallower than the in-situ
350 observations (**Table 3**). This is particularly evident for the 24 February 2021 forest lidar snow depths. The
351 lidar also has larger cell-to-cell variability than the in-situ measurements, as quantified by the standard
352 deviation, particularly in the forest. This large variability in the forest combined with the relatively small
353 range of snow depths even across sampling dates makes it nearly impossible to identify relatively shallow
354 or deep snow depths within the forest. The very low correlation values for both in-situ validation approaches
355 reflect the low signal-to-noise ratio. In contrast, there is fairly strong evidence in the field that snow depth
356 differences that exceed 3 cm are discernible.

357

358 **Fig. 7** shows that the differences between the lidar and in-situ observations, regardless of method, are
359 considerably larger than the differences between the two in-situ sampling methods. The magnaprobe's
360 potential to overprobe through leaf litter and duff layers to a greater extent than the snow tube impacts the
361 quantification of performance. Overprobing negatively impacts the bias, MAE, RMSE, and linear regression
362 intercept metrics. The RMSE values are slightly higher for the magnaprobe than the snow tube, and to a
363 large extent this reflects the higher bias when using the magnaprobe as compared to the snow tube. In
364 contrast, the snow tube's RMSE is largely due to the snow tube's high site to site differences rather than an
365 overall bias. Thus, for individual locations, the magnaprobe is more consistent in its agreement with the
366 lidar. This is also reflected in the higher R^2 value.

367 **4 Discussion**

368 **4.1 Uncertainty and impacts from overprobing**

369 This study quantifies the differences between snow depth measurements made with a magnaprobe and with a
370 Federal snow tube sampler. The differences seem to be primarily associated with greater overprobing by the
371 magnaprobe into vegetation/organic layers and thawed soils. The result was that magnaprobe snow depth
372 measurements were observed to be higher than snow tube measurements, with a greater difference in the forest
373 than the field. This result agrees with previous studies. An average of 5 cm high bias occurred in the tundra mat
374 during the Cold Land Processes Experiment (CLPX) Alaska campaign (Sturm and Holmgren 2018). A 2018
375 experiment in a single snow pit within an open tundra environment found a 7.6 cm average overprobe penetration
376 (Canada, 2018). Using a snow probe, Berezovskaya and Kane (2007) found a 5 to 9 cm bias in northern Alaska.



377 They also noted that overprobing was greater with the probe as compared to the snow tube. The current study's
378 snow-off magnaprobe forest litter depth measurements of 5.8 cm are similar to these previous finding.

379

380 Sturm and Holmgren (2018) suggested that operators need to learn to push a magnaprobe through snow yet not
381 impale it too deeply into underlying vegetation/organic layers by developing a sense for the base of the snowpack.
382 However, this recommendation could be difficult to implement over soft vegetation (e.g. tundra) where the probe
383 easily penetrates the vegetation. In that case, a consistent way to push a magnaprobe is needed by operators,
384 though any two operators will likely apply a different force (Berezovskaya and Kane 2007). If operators overprobe
385 it into the base of the (frozen) soils, one should consistently measure the depths in the same way (which would be
386 snow depth *plus* vegetation) and then subtract typical vegetation depths in the study area from the depths.
387 Measurements of leaf litter or vegetation depths may help to account for the overprobing errors of magnaprobe
388 snow depth measurements.

389

390 Overprobing also impacts SWE estimates. Given the efficiency of making snow depth measurements, a snow
391 survey will often make numerous snow depth measurements per snow density measurement then combine the
392 measurements to obtain SWE (Elder et al. 1998; López-Moreno et al. 2013). In some cases, only snow depth is
393 measured and bulk density is derived from empirical relationships. In either case, any biases in snow depth will
394 be transferred to the SWE estimates. Based on leaf litter measurements and the differences between the lidar snow
395 depth estimates and the in-situ measurements, it appears that both instruments overprobe to some extent. In fact,
396 a typical application of the snow tube will overprobe by design to extract the snow core and a “plug of soil”.
397 However, because the operator removes any vegetation and soil prior to recording measurements, snow tube
398 measurements can readily correct for the overprobing. The errors incurred by combining magnaprobe
399 measurements with snow tube density values to determine SWE likely equal or exceed those from the 1.9 cm
400 depth differences observed in this study.

401 **4.2 Recommendations for sampling strategy to validate UAS-based data**

402 To validate high-resolution snow depth measurements from UAS-based lidar and SfM photogrammetry, reliable
403 ground-based observations with an appropriate sampling strategy are required. From the surveys conducted in this
404 study, there are several technical lessons for researchers who will conduct UAS snow depth surveys.

405

406 UAS-based snow depth measurements are typically gridded outputs (1-m grid in this study). As compared to using
407 single measurements along a transect for validation, using the average of multiple-point samples within a grid can
408 reduce the point-to-point variability and spatial representativeness errors. To test if using fewer in-situ sampling
409 points makes a difference in the reported performance of the UAS Lidar measurements, the summary statistics
410 (**Table 3**) were recalculated by randomly sampling one point and three points per grid cell, respectively, and
411 extracting the paired magnaprobe and snow tube depths. In all cases, the correlations with lidar snow depth
412 degraded modestly. For example, the nine snow tube samples R^2 value of 0.40 decreased to 0.39 and 0.37 for
413 three and one sample, respectively, and the nine magnaprobe samples R^2 value of 0.53 decreased to 0.50 for both
414 three and one sample, respectively. RMSE values typically increased by 0.3 cm or less with decreasing sample



415 size. Another challenge with transect style measurements is that it is difficult to capture their locations at the
416 resolution needed to align the UAS measurements.

417

418 It may be advisable to use multiple sampling techniques, rather than a single method, in order to cross-check on
419 ground snow depth measurements because the measurement errors vary by sampling methods and surface
420 conditions (e.g. low vegetation, leaf litter, and soils), particularly in shallow snowpacks. As observed in this study,
421 leaf litter and soil frost can differentially impact in-situ snow depth sampling methods. The 3.9 cm forest leaf litter
422 depth was nearly double the 2.0 cm snow depth differences. Distinct contributions of forest leaf litter depth to
423 magnaprobe and snow tube snow depths may occur because the narrow magnaprobe fully penetrates the leaf litter
424 and the larger diameter snow tube only partially penetrates the litter, or the magnaprobe may only partially
425 penetrate the leaf litter but the snow tube does not break through the leaf litter. Partial penetration of the
426 magnaprobe into the leaf litter layer (i.e., overprobing) may vary by the freeze-thaw state of the duff layer and/or
427 mineral soil layers beneath the leaf litter layer. The horizontally aligned, matted leaf litter could also limit snow
428 tube penetration. High spatial variability of leaf litter depth could also be a factor, though this was not quantified
429 here. Thus, differences among in-situ methods in forested areas point to the particular importance of in-situ
430 validation in forested areas and, more generally, sampling with multiple methods in an area with a nonuniform
431 underlying substrate.

432

433 Emerging techniques such as automated snow depth retrievals from field cameras may offer improved validation
434 for high resolution remote sensing observations of snow status. For example, the field camera method outlined
435 above has a potential to measure snow depth consistently over time. Our preliminary results (Hunsaker et al. 2021)
436 suggest that snow depth measurements from field cameras may have better agreement with lidar-based snow
437 depths. An added advantage of field cameras is that the snowpack would not be impacted through destructive
438 measurements and foot tracks to measurement locations.

439 **4.3 Future perspectives**

440 While airborne-based lidar and SfM photogrammetry have been widely used to generate spatially distributed snow
441 depth maps at scales between ground measurements and satellite or regional snow products (Deems et al. 2013;
442 Painter et al. 2016), the airborne systems have limited availability for repeated deployments over a season due to
443 costs, limiting its use for many studies. For field-scale hydrological and ecological research where higher spatial
444 and temporal resolution snow information are needed, UAS-based lidar and SfM platforms can bridge between
445 ground measurements and the airborne-based information (Cho et al. 2021). Due to the economic feasibility and
446 availability of deployment, these systems are increasingly being used and have potentials to advance snow science.
447 For example, the extent and periods of shallow and ephemeral snowpack will likely increase in a warmer climate
448 making accurate measurements increasingly (Siirila-Woodburn et al. 2021) important. The UAS observations may
449 also allow small changes in deeper snowpacks to be observed and, in turn, offer improved understanding of the
450 snowpack accumulation, ablation, and redistribution. However, as remotely sensed observations or model outputs
451 continue to improve the ability to estimate snow depth, we appear to be reaching current limits to validate those
452 improvements.

453



454 The current results provide further support for previous studies that articulated the limits of in-situ observations.
455 For snow study, the UAS lidar-based measurements may be more representative of snowpack conditions than the
456 point sampling observations used to validate other remotely sensed and modelled snow products. At the same
457 time, we expect that magnaprobes, or similar high efficiency snow depth measuring techniques, will continue to
458 be needed for validation of remote sensing and model estimates as an essential and consistent approach. Further
459 studies in other environments with different vegetation and soil conditions would help to minimize the errors from
460 in-situ sampling and improve the needed validation of the UAS snow depth maps.

461 **5 Conclusion**

462 Manual in situ sampling snow depth measurements can be made quickly and easily, but making consistent,
463 representative, and unbiased measurements can be challenging when the surface is irregular, vegetation/organic
464 layers and unfrozen soils result in overprobing, and the leaf litter compacts during the winter. This study quantified
465 the differences between snow depth measurements made with a magnaprobe and a Federal snow tube and assessed
466 impacts on the validation of UAS lidar-based snow depth measurements in a mixed-use temperate forest landscape
467 with ephemeral snowpack. For all sampling campaigns and land cover types, the magnaprobe snow depth
468 measurements (mean 14.9 cm) were consistently deeper than the snow tube measurements (13.2 cm), which was
469 a 12% average difference with a greater difference in the forest than the field. The lidar-based snow depths were
470 shallower than the magnaprobe and snow tube measurements by 3.6 cm and 1.9 cm on average, respectively.
471 RMSE values between the magnaprobe and the lidar snow depths (3.6 and 5.4 cm) were larger than that between
472 the snow tube and the lidar (3.2 and 4.4 cm for field and forest, respectively) partially due to overprobing by the
473 magnaprobe into leaf litter and surface soils. For a robust validation of the UAS lidar and SfM-based snow depth
474 maps, there are several suggestions for those who conduct similar studies.

- 475 1) For validation of the lidar snow depths, the use of the average of multiple-point samples within a grid is
476 recommended instead of single measurements, because the average of multiple-point samples can reduce the
477 point-to-point variability and spatial representativeness errors.
- 478 2) Measurements of leaf litter and soil frost may help to account for the overprobing errors, particularly when
479 using a magnaprobe.
- 480 3) To cross-check on ground snow depth measurements, the use of multiple sampling techniques is highly
481 recommended (rather than a single method) because the measurement errors vary by sampling methods and
482 surface conditions (e.g., low vegetation, leaf litter, and soils), particularly in shallow snowpacks.

483 As the UAS lidar or optical systems are increasingly used in snow research, it is prudent to recognize that snow
484 depth maps produced by these remote sensing products are likely to be modestly shallower than coincident in situ
485 observations. The differences among measurement techniques in this present study reflect the current study area,
486 surface conditions for a single season, and the operation of the instruments by this project team. Further studies
487 to minimize the errors from in-situ sampling in various snow environments in with different vegetation and soil
488 conditions are needed to accurately validate UAS snow depth maps and to provide guidance on best practices for
489 using these maps in combination with in situ measurements to represent differences in snow depth and SWE over
490 space and time.



491 **Acknowledgements**

492 This material is based upon work supported by the Broad Agency Announcement Program and the Cold Regions
493 Research and Engineering Laboratory (ERDC-CRREL) under Contract No. W913E518C0005 and
494 W913E521C0006. The authors are grateful to Lee Friess for providing a technical review of the draft manuscript,
495 Mahsa Moradi Khaneghahi for supporting manuscript preparation, and Brigid Ferris for training the team on litter
496 depth sampling.

497 **Data Availability**

498 The UAS-based lidar point clouds and in-situ snow observations are available from the corresponding author upon
499 reasonable request.

500 **Author Contributions**

501 HP, JJ, EB, AH, FS, MP, and EC designed the research. HP, CW, JJ, AH, FS, MP, EB, and EC conducted field
502 work to obtain lidar and/or in-situ snow observations. HP, CW, JJ, EB, AH, and MP performed the analysis.
503 HP, EC, and AH produced the figures. HP, JJ, EB, and EC wrote the initial draft. All authors contributed to
504 manuscript review and editing.

505 **Competing Interests**

506 The authors declare that they have no conflict of interest.

507 **References**

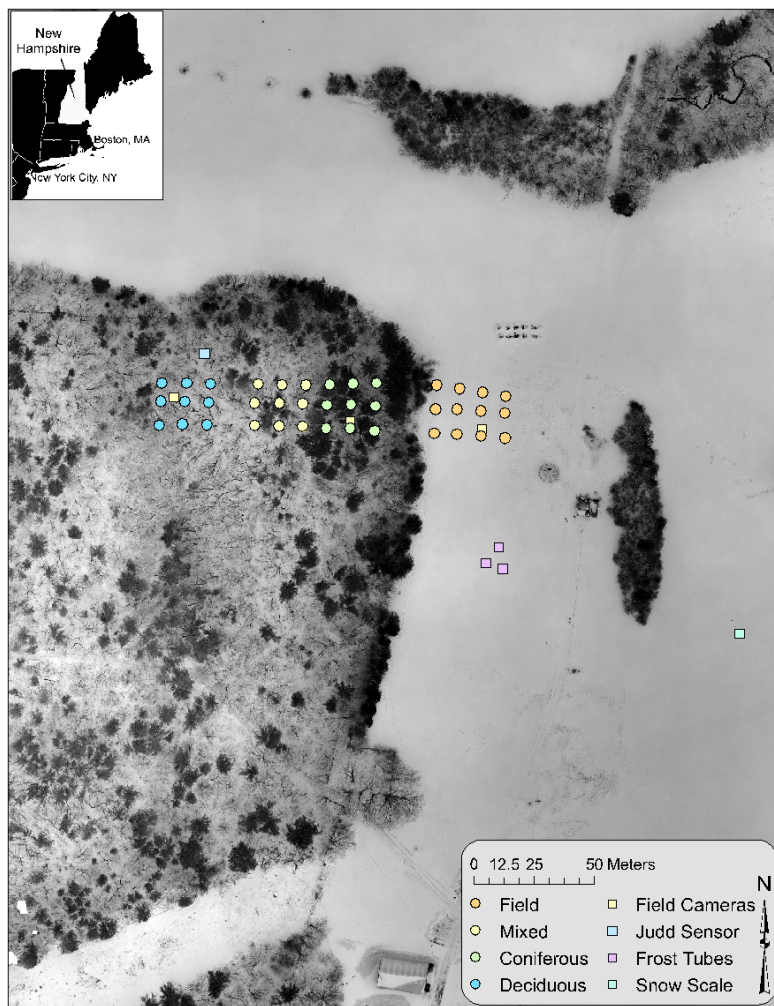
- 508 Berezovskaya, S., and D. L. Kane, 2007: Measuring snow water equivalent for hydrological applications: part 1,
509 accuracy of observations. *Proceedings of the 16 th International Northern Research Basins Symposium and*
510 *Workshop, Petrozavodsk, Russia*, 29-37.
- 511 Bühler, Y., M. S. Adams, R. Bösch, and A. Stoffel, 2016: Mapping snow depth in alpine terrain with unmanned
512 aerial systems (UASs): potential and limitations. *The Cryosphere*, **10**, 1075-1088.
- 513 Burakowski, E., and Coauthors, 2018: The role of surface roughness, albedo, and Bowen ratio on ecosystem
514 energy balance in the Eastern United States. *Agricultural and Forest Meteorology*, **249**, 367-376.
- 515 Burakowski, E. A., and Coauthors, 2015: Spatial scaling of reflectance and surface albedo over a mixed-use,
516 temperate forest landscape during snow-covered periods. *Remote Sensing of Environment*, **158**, 465-477.
- 517 Cho, E., A. G. Hunsaker, J. M. Jacobs, M. Palace, F. B. Sullivan, and E. A. Burakowski, 2021: Maximum entropy
518 modeling to identify physical drivers of shallow snowpack heterogeneity using unpiloted aerial system (UAS)
519 lidar. *Journal of Hydrology*, **602**, 126722.
- 520 Clyde, G. D., 1932: Utah snow sampler and scales for measuring water content of snow.
- 521 Currier, W. R., and Coauthors, 2019: Comparing aerial lidar observations with terrestrial lidar and snow-probe
522 transects from NASA's 2017 SnowEx campaign. *Water Resources Research*.
- 523 Deems, J. S., T. H. Painter, and D. C. Finnegan, 2013: Lidar measurement of snow depth: a review. *J. Glaciol.*,
524 **59**, 467-479.
- 525 Derry, J., D. Kane, M. Lilly, and H. Toniolo, 2009: Snow-course measurement methods, North Slope, Alaska.
526 *University of Alaska Fairbanks, Water and Environmental Research Center, Report INE/WERC*, **15**.
- 527 Elder, K., W. Rosenthal, and R. E. Davis, 1998: Estimating the spatial distribution of snow water equivalence in
528 a montane watershed. *Hydrological Processes*, **12**, 1793-1808.
- 529 Farnes, P. E., B. E. Goodison, N. R. Peterson, and R. P. Richards, 1983: Metrication of manual snow sampling
530 equipment. *Final report Western Snow Conference*, 19-21.



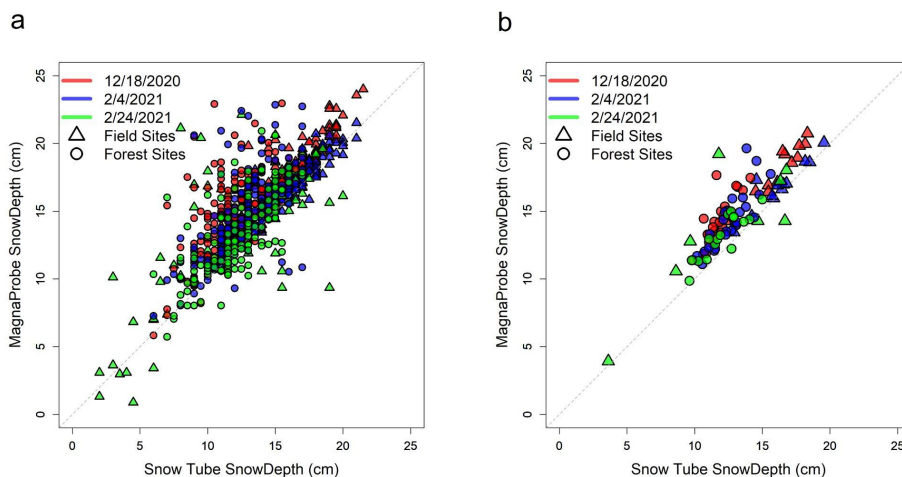
- 531 Gandahl, R., 1957: Determination of the depth of soil freezing with a new frost meter. *Text in Swedish) Rapport*,
532 **20**, 3-15.
- 533 Grünwald, T., and M. Lehning, 2015: Are flat-field snow depth measurements representative? A comparison of
534 selected index sites with areal snow depth measurements at the small catchment scale. *Hydrological Processes*,
535 **29**, 1717-1728.
- 536 Guyennon, N., M. Valt, F. Salerno, A. B. Petrangeli, and E. Romano, 2019: Estimating the snow water equivalent
537 from snow depth measurements in the Italian Alps. *Cold Regions Science and Technology*, **167**, 102859.
- 538 Harder, P., J. W. Pomeroy, and W. D. Helgason, 2020: Improving sub-canopy snow depth mapping with
539 unmanned aerial vehicles: lidar versus structure-from-motion techniques. *The Cryosphere*, **14**, 1919-1935.
- 540 Harder, P., M. Schirmer, J. Pomeroy, and W. Helgason, 2016: Accuracy of snow depth estimation in mountain
541 and prairie environments by an unmanned aerial vehicle. *The Cryosphere*, **10**, 2559.
- 542 Hill, D. F., and Coauthors, 2019: Converting snow depth to snow water equivalent using climatological variables.
543 *The Cryosphere*, **13**, 1767-1784.
- 544 Hopkinson, C., L. Chasmer, C. Young-Pow, and P. Treitz, 2004: Assessing forest metrics with a ground-based
545 scanning lidar. *Canadian Journal of Forest Research*, **34**, 573-583.
- 546 Hunsaker, A., and Coauthors, 2021: Unpiloted Aerial Systems (UAS) Lidar and Photogrammetry to Estimate
547 Snow Depth and Snow Covered Area *AGU Fall Meeting Abstracts*.
- 548 Jacobs, J. M., A. G. Hunsaker, F. B. Sullivan, M. Palace, E. A. Burakowski, C. Herrick, and E. Cho, 2021: Snow
549 depth mapping with unpiloted aerial system lidar observations: a case study in Durham, New Hampshire, United
550 States. *The Cryosphere*, **15**, 1485-1500.
- 551 Jonas, T., C. Marty, and J. Magnusson, 2009: Estimating the snow water equivalent from snow depth
552 measurements in the Swiss Alps. *Journal of Hydrology*, **378**, 161-167.
- 553 Kaspari, M., and S. P. Yanoviak, 2008: Biogeography of litter depth in tropical forests: evaluating the phosphorus
554 growth rate hypothesis. *Functional Ecology*, **22**, 919-923.
- 555 Kinar, N., and J. Pomeroy, 2015: Measurement of the physical properties of the snowpack. *Rev. Geophys.*, **53**,
556 481-544.
- 557 Kopp, M., Y. Tuo, and M. Disse, 2019: Fully automated snow depth measurements from time-lapse images
558 applying a convolutional neural network. *Science of The Total Environment*, **697**, 134213.
- 559 Leppänen, L., A. Kontu, H.-R. Hannula, H. Sjöblom, and J. Pulliainen, 2016: Sodankylä manual snow survey
560 program. *Geoscientific Instrumentation, Methods and Data Systems*, **5**, 163-179.
- 561 López-Moreno, J. I., and Coauthors, 2013: Small scale spatial variability of snow density and depth over complex
562 alpine terrain: Implications for estimating snow water equivalent. *Advances in water resources*, **55**, 40-52.
- 563 Muir, J., N. Goodwin, J. Armston, S. Phinn, and P. Scarth, 2017: An accuracy assessment of derived digital
564 elevation models from terrestrial laser scanning in a sub-tropical forested environment. *Remote Sensing*, **9**, 843.
- 565 Nolan, M., C. Larsen, and M. Sturm, 2015: Mapping snow-depth from manned-aircraft on landscape scales at
566 centimeter resolution using Structure-from-Motion photogrammetry. *Cryosphere Discussions*, **9**.
- 567 Painter, T. H., and Coauthors, 2016: The Airborne Snow Observatory: Fusion of scanning lidar, imaging
568 spectrometer, and physically-based modeling for mapping snow water equivalent and snow albedo. *Remote
569 Sensing of Environment*, **184**, 139-152.
- 570 Perron, C. J., K. Bennett, and T. D. Lee, 2004: Forest stewardship plan: Thompson farm. NH:
571 University of New Hampshire. Ossipee Mountain Land Company, West Ossipee.
572 <https://colsa.unh.edu/sites/default/files/thompson-farm-plan.pdf>.
- 573 Pirazzini, R., and Coauthors, 2018: European in-situ snow measurements: Practices and purposes. *Sensors*, **18**,
574 2016.
- 575 Ricard, J., W. Tobiasson, and A. Greatorex, 1976: The field assembled frost gage. U.S. Army Corps of Engineers
576 Cold Regions Research and Engineering Laboratory (CRREL). Hanover, NH.
- 577 Rickard, W., and J. Brown, 1972: The performance of a frost-tube for the determination of soil freezing and
578 thawing depths. *Soil science*, **113**, 149-154.
- 579 Rovaneck, R., D. Kane, and L. Hinzman, 1993: Improving estimates of snowpack water equivalent using double
580 sampling. *Proceedings of the 61st Western snow conference*, 157-163.
- 581 Sharratt, B. S., and D. K. McCool, 2005: Frost depth.
- 582 Siirila-Woodburn, E. R., and Coauthors, 2021: A low-to-no snow future and its impacts on water resources in the
583 western United States. *Nature Reviews Earth & Environment*, **2**, 800-819.
- 584 Sturm, M., and J. Holmgren, 2018: An automatic snow depth probe for field validation campaigns. *Water
585 Resources Research*, **54**, 9695-9701.
- 586 Sturm, M., B. Taras, G. E. Liston, C. Derksen, T. Jonas, and J. Lea, 2010: Estimating snow water equivalent using
587 snow depth data and climate classes. *Journal of Hydrometeorology*, **11**, 1380-1394.
- 588 Walker, B., E. J. Wilcox, and P. Marsh, 2020: Accuracy assessment of late winter snow depth mapping for tundra
589 environments using Structure-from-Motion photogrammetry. *Arctic Science*, 1-17.



590 Willmott, C. J., 1982: Some comments on the evaluation of model performance. *Bulletin of the American*
591 *Meteorological Society*, **63**, 1309-1313.
592



593
594 **Figure 1:** The 4 February 2021 aerial optical image of Thompson Farm, Durham NH, USA showing both forest
595 and field region with snow sampling sites in the field, coniferous, mixed, and deciduous forested areas as well as
596 the locations of the CRREL-Gandahl soil frost tubes; and field cameras.

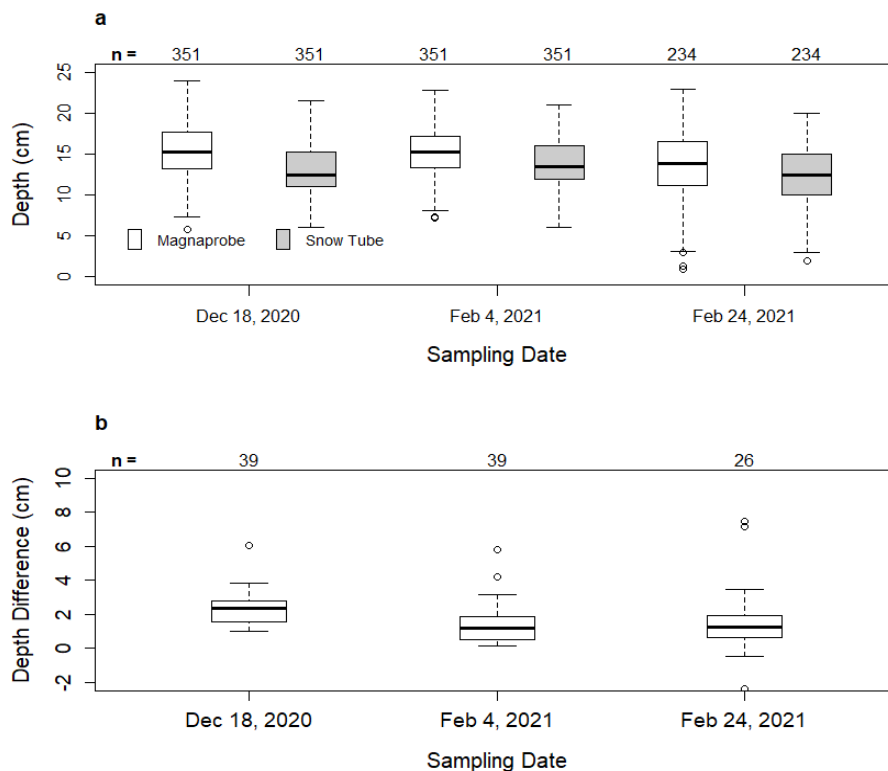


597

598

599

Figure 2: Comparison of snow depths measured by magnaprobe and snow tube for the three sampling campaigns using (a) the sampling individual points ($n = 936$) and (b) using grid cell average values ($n=104$).



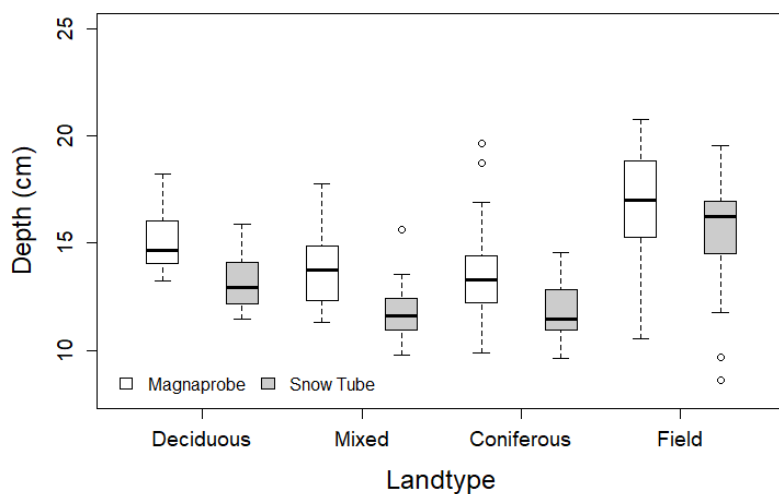
600

601

602

603

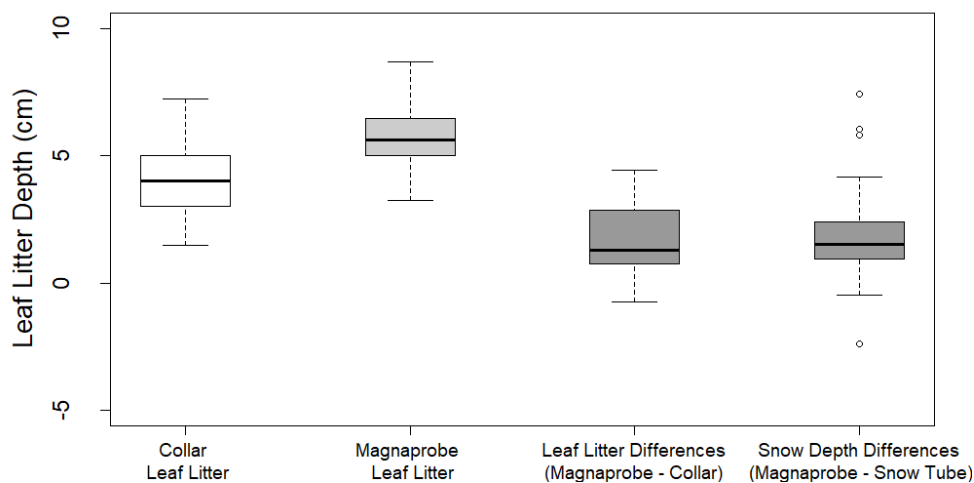
Figure 3: Boxplots of snow depths measured by magnaprobe and snow tube for the three sampling campaigns using (a) all the grid values and (b) differences between grid cell average values by date where n is the number of (a) sample points and (b) sample grids.



604

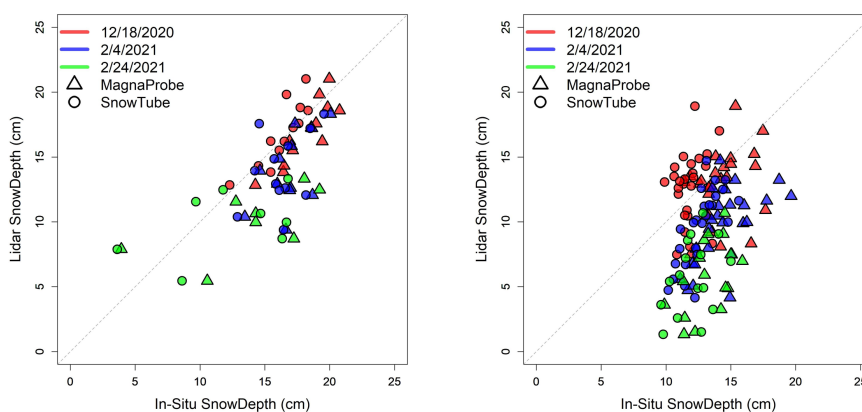
605 **Figure 4:** Boxplots of snow depths by land type measured by the magnaprobe and the snow tube for the three
 606 sampling campaigns using the grid cell average values.

607



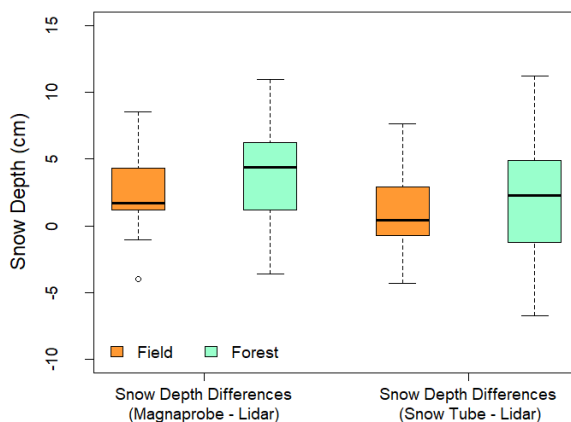
608

609 **Figure 5:** Boxplots of leaf litter depth measurements taking under snow free conditions on 2 April 2021 by the
 610 leaf litter collar technique and the snow off magnaprobe technique, as compared to boxplots of litter depth
 611 differences as measured by collar and magnaprobe techniques, and snow depth differences measured by
 612 magnaprobe and snow tube for the three sampling campaigns using the grid cell average values in the forest.



613
 614
 615
 616

Figure 6: Comparison of 1 m grid cell average snow depths measured by the magnaprobe and snow tube versus the UAS lidar for the three sampling campaigns in the field (left) and the forest (right).



617
 618
 619
 620

Figure 7: Difference of 1 m grid cell average snow depths measured by the magnaprobe and lidar for the three sampling campaigns in the field and the forest.

Table 1: Summary of snow and soil frost conditions during the winter 2020/2021 field campaigns at Thompson Farm, Durham NH. Snow depth was measured from field cameras.

Variables	Land type	Campaign Date		
		18 December	4 February	24 February
Snow Depth (cm)	Field	10	12.5	15
	Forest	9.8	10.8	9.3
Snow Density (g/cm ³)	Field	0.09	0.15	0.24
	Forest	0.10	0.15	0.20
Soil Frost (cm)	Field	3.7	15.1	13.8
	Forest	2.2	5.9	2.1



623 **Table 2:** Summarized statistics of snow depths for the magnaprobe and snow tube techniques by the individual
 624 points and the grid cell averaged values for each of the sampling campaign dates. All units are cm except slope
 625 and R^2 , which are dimensionless.

Date	Magnaprobe Mean (Std)	Snow tube Mean (Std)	Bias	N	Intercept	Slope	R^2	MAE	RMSE
All Measurements									
18 December	15.5 (3.1)	13.2 (2.9)	2.3	351	1.85	0.73	0.62	2.4	3.0
4 February	15.2 (2.8)	13.9 (2.7)	1.4	351	2.70	0.73	0.59	1.6	2.3
24 February	13.6 (3.8)	12.2 (3.4)	1.4	234	4.29	0.58	0.43	2.2	3.3
All Dates	14.9 (3.3)	13.2 (3.0)	1.7	936	3.09	0.68	0.55	2.0	2.9
Grid Cell Averages									
18 December	15.5 (2.6)	13.3 (2.5)	2.3	39	-0.67	0.90	0.85	2.3	2.5
4 February	15.2 (2.3)	13.8 (2.3)	1.4	39	0.71	0.86	0.74	1.4	1.8
24 February	13.6 (3.0)	12.2 (2.7)	1.4	26	2.05	0.74	0.66	1.7	2.3
All Dates	14.9 (2.7)	13.2 (2.5)	1.7	104	0.91	0.82	0.75	1.8	2.2

626

627 **Table 3:** Summary statistics of 1 m grid cell average snow depth values for the lidar as compared to the in-situ
 628 magnaprobe and snow tube separated into forest and field locations. All units are cm except slope and R^2 , which
 629 are dimensionless.

Land type	Technique	In-situ Mean (Std)	Lidar Mean (Std)	Bias	N	Intercept	Slope	R^2	MAE	RMSE
Field	Magnaprobe	16.6 (3.3)	14.1 (3.7)	2.5	32	0.38	0.82	0.53	2.9	3.6
	Snow Tube	15.3 (3.2)		1.2	32	2.98	0.72	0.40	2.4	3.2
Forest	Magnaprobe	14.1 (1.9)	9.9 (3.9)	4.2	66	-3.28	0.94	0.21	4.5	5.4
	Snow Tube	12.2 (1.3)		2.3	66	0.74	0.75	0.07	3.6	4.4

630